Biogeochemical controls on photic-zone euxinia during the end-Permian mass extinction

K.M. Meyer[1], L.R. Kump[1], A. Ridgwell[2]
[1]Department of Geosciences, Pennsylvania State University, University Park, Pennsylvania 16802, USA
[2]School of Geographical Sciences, University of Bristol, Bristol BS8 1SS, UK

ABSTRACT

Geochemical, biomarker, and isotopic evidence suggests that the end-Permian was characterized by extreme oceanic anoxia that may have led to hydrogen sulfide buildup and mass extinction. We use an earth system model to quantify the biogeochemical and physical conditions necessary for widespread oceanic euxinia and hydrogen sulfide release to the atmosphere. Greater than threefold increases in ocean nutrient content combined with nutrient-trapping ocean circulation cause surface-water H_2S accumulation in the paleo–Tethys Ocean and in areas of strong upwelling. Accounting for the presence of sulfide-oxidizing phototrophs in the model suppresses but does not prevent widespread release of H_2S to the atmosphere. Evidence from the geologic record is consistent with modeled geochemical distributions of widespread nutrient-induced euxinia during the end-Permian, suggesting H_2S toxicity and hypercapnia may have provided the kill mechanism for extinction.

Keywords: Permian-Triassic boundary, mass extinction, euxinia, hydrogen sulfide, earth system model, anoxia.

INTRODUCTION

The largest of the Phanerozoic mass extinctions marked the close of the Permian Period. This event impacted marine and terrestrial ecosystems with species-level extinction estimates over 90% (Erwin, 2006). The cause of the extinction remains controversial, although most hypotheses invoke geographic, environmental, or climatic explanations (e.g., Berner, 2005; Hallam and Wignall, 1999; Huey and Ward, 2005; Isozaki, 1997; Knoll et al., 1996; Krull and Retallack, 2000; Kump et al., 2005; Newton et al., 2004; Renne and Basu, 1991; Wignall and Twitchett, 1996). Ocean stagnation, anoxia, and euxinia (anoxic and sulfidic conditions) have been linked to end-Permian mass extinction in several of these hypotheses.

Multiple lines of evidence support the notion that the world's oceans became anoxic, and possibly euxinic, during the Late Permian. Dark, laminated cherts from Japan and British Columbia suggest a brief episode of euxinia during the extinction punctuated a prolonged interval of Panthalassic anoxia (Isozaki, 1997). Framboidal pyrite size distribution in rocks from China, Greenland, and India suggest a sulfidic water column (Algeo et al., 2007; Nielsen and Shen, 2004; Wignall et al., 2005). Large shifts in the $\delta^{34}S$ composition of carbonate-associated sulfate and pyrite indicate a perturbation to the Tethyan, and perhaps global, sulfur cycle (Newton et al., 2004; Riccardi et al., 2006). Also, in the paleo–Tethys Ocean, excursions in the $\delta^{13}C_{carb}$ record persist through the Early Triassic (Payne et al., 2004), and unusual aragonite fans and microbial carbonates may be a result of CO_2 degassing from upwelling euxinic deep waters (Knoll et al., 1996; Pruss and Bottjer, 2004). Compelling evidence for euxinic conditions lies in the identification of biomarkers for photic-zone euxinia from sediments in China, Australia, and Greenland (Grice et al., 2005; Hays et al., 2006).

Previous work has demonstrated that Permian ocean stagnation is unlikely (Hotinski et al., 2001; Winguth and Maier-Reimer, 2005), but a more sluggish circulation is possible (Kiehl and Shields, 2005). Instead, Kump et al. (2005) proposed that warming from Siberian trap volcanism forced earth system feedbacks that led to euxinia. In this scenario, high pCO_2 and an intensified hydrologic cycle stimulated continental weathering and enhanced phosphate delivery to the ocean. Upwelling of PO_4^{3-}-enriched deep water supported higher export productivity and led to greater oxygen demand in the deep ocean, and anoxia spread. Bacterial sulfate reduction in anoxic waters produced H_2S and deep-ocean euxinia. Euxinia led to reduced phosphate burial and phosphate liberation from surface sediments, further stimulating new production in a euxinia-enhancing positive feedback (Van Cappellen and Ingall, 1994). Basins with estuarine-like circulation acted as nutrient traps; these are systems in which PO_4^{3-}-rich deep waters were imported and PO_4^{3-}-depleted surface waters exited the basin (Demaison and Moore, 1980). The ultimate result was increasing general eutrophication of a sulfidic ocean and strong euxinia in nutrient-trapping basins (Meyer and Kump, 2008).

Simple back-of-the-envelope calculations show that photic-zone euxinia would have resulted if the ratio of deep-water H_2S to atmospheric pO_2 reached a critical threshold (Kump et al., 2005). Hydrogen sulfide release to the atmosphere would have followed, and one-dimensional (1-D) modeling has predicted that high sulfide fluxes could cause loss of ozone, leading to drastic radiative impacts on land (Kump et al., 2005). Subsequent two-dimensional (2-D; Beerling et al., 2007) and three-dimensional (3-D; Lamarque et al., 2007) atmospheric photochemical modeling of the consequences of similar H_2S fluxes generated lower tropospheric H_2S levels than predicted by Kump et al. (2005), and, consequently, lesser effects on atmospheric ozone and methane. The ppm levels of tropospheric H_2S predicted by the 3-D models would likely create chronic rather than acute stress on the terrestrial biota.

Here, we use an earth system model of intermediate complexity to more realistically investigate the physical and biogeochemical conditions necessary to achieve photic-zone euxinia in the end-Permian ocean. We examine the amount, distribution, and ocean-atmosphere flux of H_2S under a range of oceanic nutrient conditions. Additionally, we consider the role that sulfur phototrophs might have played in suppressing the buildup of H_2S in surface waters. We compare our spatially resolved predictions to key observations from the geologic record and the Permian-Triassic (P-T) boundary extinction pattern.

MODEL DESCRIPTION

We used the GENIE-1 earth system model (Ridgwell et al., 2007) to examine the buildup of euxinia in the end-Permian ocean. GENIE-1 consists of a 3-D non-eddy resolving frictional geostrophic ocean circulation

model coupled to a 2-D energy moisture balance atmospheric model (Edwards and Marsh, 2005). The ocean model is based on a 36 × 36 equal-area horizontal grid with eight vertical levels. GENIE-1 is computationally efficient (~1000 model years per hour on a conventional processor), and it is capable of performing multiple simulations over the long intervals that are relevant to the time scale of end-Permian mass extinction (~400 k.y.; Mundil et al., 2004). The GENIE-1 model also incorporates a representation of the marine geochemical cycling of carbon and other biologically mediated tracers (fully described in Ridgwell et al., 2007; see also the GSA Data Repository[1]). To our knowledge, this is the first coupled climate–carbon cycle model capable of simulating carbon and sulfur cycling in an anoxic ocean.

We configured the GENIE-1 model explicitly for the end-Permian using the paleogeography, paleobathymetry, and wind stress fields equilibrated in the 12× PAL (pre-industrial atmospheric level) pCO_2 atmosphere of Kiehl and Shields (2005; Fig. 1A). We also specified 12× PAL atmospheric pCO_2, which is within the range of estimates for this interval and results in an ice-free world (Kidder and Worsley, 2004; Kiehl and Shields, 2005). All simulations used an atmosphere containing 0.2095 atm O_2, so these results are likely minima for the spread of anoxia and euxinia, presuming that atmospheric oxygen levels were on the decline at that time (Berner, 2005).

Using the end-Permian configuration, we ran a series of model simulations until they achieved equilibrium (~10,000 model years). For the first set of runs, we increased oceanic phosphate from modern to 10× modern levels in increments of the modern phosphate content. In a second set, we added the metabolic effect of sulfur phototrophs to the surface ocean and performed an otherwise identical series of simulations. Here, we examine the biogeochemical causes of the transition to euxinia, detail the spatial distribution of euxinia for comparison to the rock record, and quantify the impact of sulfur phototrophy upon surface-water H_2S concentration.

RESULTS

End-Permian model simulations predict an ice-free world with sea-surface temperatures as high as 34 °C, consistent with previous modeling (Kiehl and Shields, 2005). Despite these warm temperatures, the oceans remain well oxygenated at modern nutrient levels. A pronounced oxygen minimum zone (OMZ) develops in the paleo–Tethys Ocean, and oxygen concentrations ($[O_2]$) decrease below 1 μM. Consistent with Hotinksi et al. (2001), $[O_2]$ remains above ~150 μmol kg^{-1} throughout the Panthalassic Ocean. In contrast, simulations by Winguth and Maier-Reimer (2005) displayed a Panthalassic OMZ with $[O_2]$ as low as 20 μmol kg^{-1}. Their greater modeled export production created elevated oxygen demand and thus relatively low $[O_2]$ at depth, especially in productive regions. No H_2S is observed in the world's oceans with present-day nutrient conditions in GENIE-1.

In GENIE-1 overturning circulation is roughly symmetrical across the equator with a meridional transport of 20–25 Sverdrups (1 Sv = 10^6 m^3 s^{-1}). The pattern of transport is similar to that of Hotinski et al. (2001) and Kiehl and Shields (2005). Circulation strength is comparable to Hotinski et al. (2001) and within the range of several other models (Kiehl and Shields, 2005; Winguth and Maier-Reimer, 2005). Additional model detail is available in the GSA Data Repository (Figs. DR1–DR11).

Simulations with elevated nutrient content demonstrate the predicted relationship between nutrient-limited export production and sulfide accumulation. H_2S first appears at the location of the present-day OMZ and then spreads to deep water in the mid-latitudes. A doubling of PO_4^{3-} induces deep-water $[H_2S]$ greater than 100 μmol kg^{-1} in the paleo–Tethys Ocean.

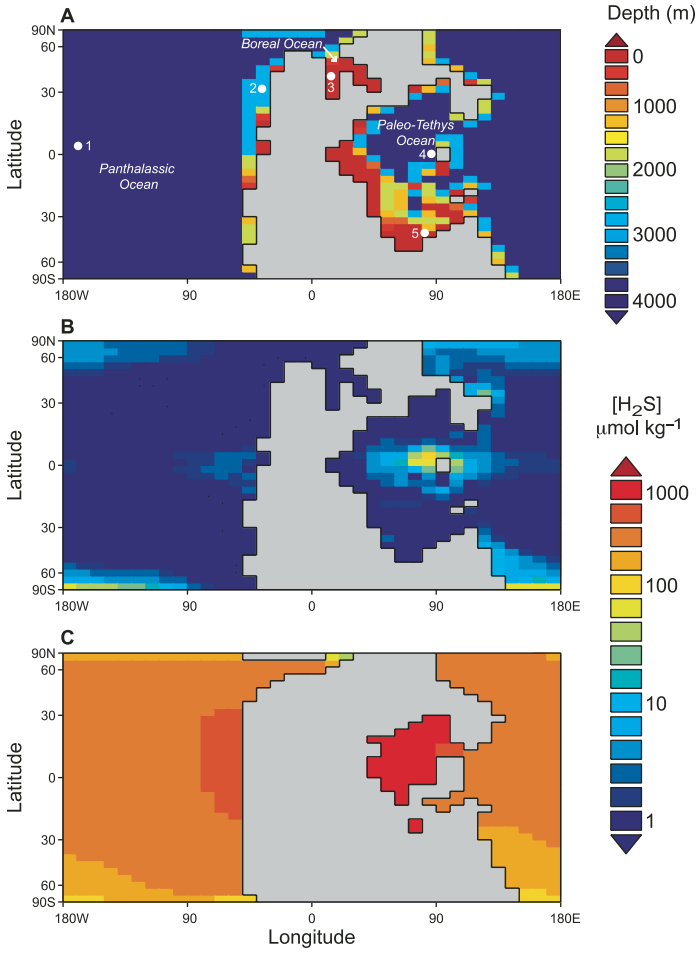

Figure 1. A: Bathymetry used in end-Permian GENIE simulations. Locations referred to in text are labeled here: 1—Japan, 2—British Columbia, 3—East Greenland, 4—South China, 5—Australia. For a complete discussion of end-Permian paleogeography, refer to Wignall and Twitchett (2002). B: Distribution of modeled surface-water hydrogen sulfide concentrations from a simulation with 10× modern oceanic phosphate levels. C: Distribution of deep-water hydrogen sulfide concentrations at ~3500 m depth from same simulation shown in B. These values are consistent with calculations by Knoll et al. (1996).

Upwelling delivers nutrient-rich, sulfidic deep water to the surface ocean. Where the upward sulfide flux exceeds the downward wind-mixed oxygen flux, H_2S persists in surface waters, as predicted by Kump et al. (2005). In the surface ocean surrounding South China, $[H_2S]$ exceeds 1 μmol kg^{-1} as a result of tripling oceanic phosphate. If the value is increased from 3× to 10× modern $[PO_4^{3-}]$, sulfidic regions of the surface ocean expand to include a majority of the paleo–Tethys Ocean as well as coastal and equatorial upwelling areas of the Panthalassic Ocean. At 10× modern $[PO_4^{3-}]$, all but shallow, wind-mixed areas of the ocean become sulfidic (Figs. 1B and 1C). Simulations that include sulfur phototrophy show as much as a 25% reduction in surface layer $[H_2S]$ (Fig. 2). Falling atmospheric pO_2 across the Permian-Triassic boundary may have sustained euxinic conditions despite biological sulfide oxidation after the initial volcanic forcing ceased.

Why do both the surface and deep paleo-Tethys exhibit higher $[H_2S]$ than the Panthalassic Ocean? Figure 3 depicts the elevated deep-water paleo-Tethys $[PO_4^{3-}]$ relative to Panthalassic deep waters. Our simulations show surface waters are exported from the paleo–Tethys Ocean, while nutrient-rich deep waters are imported; this circulation pattern increases basinwide nutrient levels. Therefore, the observed H_2S distribution is con-

[1]GSA Data Repository item 2008187, detailed model description and additional model results, is available online at www.geosociety.org/pubs/ft2008.htm, or on request from editing@geosociety.org or Documents Secretary, GSA, P.O. Box 9140, Boulder, CO 80301, USA.

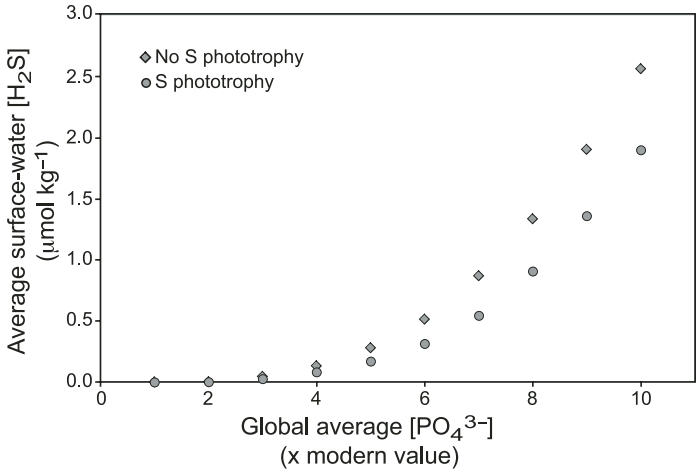

Figure 2. Average surface-water hydrogen sulfide concentration plotted against oceanic phosphate content. Metabolic activities of sulfur phototrophs are included in simulations represented by circles and are excluded from simulations represented by diamonds.

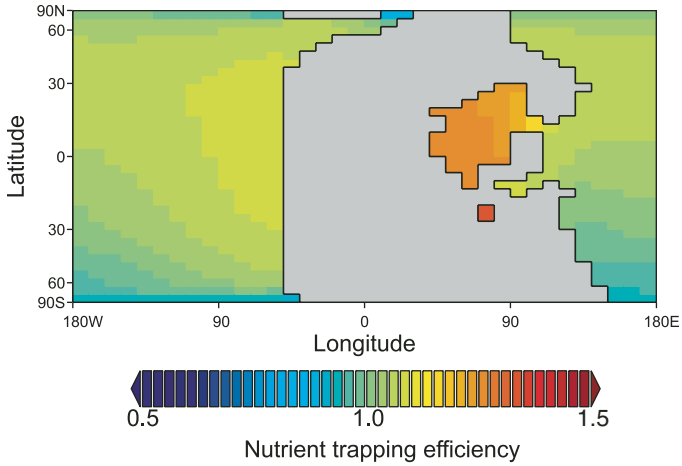

Figure 3. Modeled nutrient trapping efficiency of end-Permian bottom water. Nutrient trapping efficiency is defined here as $[PO_4^{3-}]/[PO_4^{3-}]_{global\ average}$.

sistent with sulfide focusing in upwelling regions and is enhanced by the paleo-Tethys nutrient trap (Meyer and Kump, 2008).

As the extent and concentration of H_2S in surface waters increase, the H_2S flux to the atmosphere increases with a relationship that essentially parallels the trend seen in Figure 2. At 3× modern phosphate content with S phototrophs present, the H_2S flux exceeds the modern volcanic value of 2 Tg S yr^{-1}. At 10× $[PO_4^{3-}]$, the H_2S release is nearly 4000 Tg S yr^{-1}.

RELATIONSHIP TO ROCK RECORD AND EXTINCTION

Our results are in broad agreement with geologic observations. Geochemical and sedimentological data suggest that widespread Panthalassic dysoxia began during the Changxingian, and anoxic waters spread to most of the world's oceans by the end of the Permian. By the time of the Permian-Triassic boundary, only the southern margin of the neo–Tethys Ocean shows evidence for oxic deposition (Wignall and Twitchett, 2002). Additionally, biomarker evidence from South China, Western Australia, and British Columbia indicates H_2S in the photic zone near the Permian-Triassic boundary (Grice et al., 2005; Hays et al., 2007). Large shifts in $\delta^{13}C$ and $\delta^{34}S$ in South China link disturbances to marine carbon and sulfur cycles, consistent with transition to euxinia (Newton et al., 2004; Payne et al., 2004; Riccardi et al., 2006). Evidence for oceanic anoxia or euxinia persists through the mid-Griesbachian, finally giving way to oxygenation in the mid-Dienerian (Wignall and Twitchett, 2002).

Our model results both confirm the evidence for water-column sulfide and place constraints on end-Permian nutrient conditions. At 3× modern $[PO_4^{3-}]$, dysoxic bottom waters appear widespread in Panthalassa, while $[H_2S]$ accumulates to ~130 µmol kg^{-1} below 400 m water depth in the paleo–Tethys Ocean. The upper portion of the Panthalassic water column remains well oxygenated. This observation is consistent with initial dysoxia in the Panthalassic Ocean (Isozaki, 1997) followed by latest Permian euxinia in the shallow paleo–Tethys Ocean (Wignall and Twitchett, 2002), since deep-basin facies (below 400 m) are not well represented in Tethyan sections. This pattern is also consistent with an offshore to nearshore progression of the bryozoan extinction over the course of the latest Permian (Powers and Bottjer, 2007).

With increasing $[PO_4^{3-}]$, the onset of photic-zone euxinia in the modeled paleo–Tethys Ocean coincides with deep-water euxinia in the Panthalassic Ocean. The paleo-Tethys nutrient trap results in sulfidic deep water (greater than 1200 µmol kg^{-1}) and the expression of high surface-water $[H_2S]$ at 10× $[PO_4^{3-}]$, especially near South China (Fig. 1B). H_2S is widespread throughout intermediate and deep waters worldwide. Wind mixing along the shallow southern margin of the neo–Tethys Ocean prevents the development of anoxic or sulfidic conditions, consistent with local oxic deposition through the Permian-Triassic boundary (Wignall and Twitchett, 2002).

Modeled and observed ocean conditions are in conflict for the Boreal Ocean. Biomarker evidence (Hays et al., 2006) and framboidal pyrite evidence (Nielsen and Shen, 2004) indicate a sulfidic water column, but the area remains oxic in GENIE simulations. This is likely due to the coarse resolution of the model in which the Boreal Ocean is only one layer deep.

Our results support the hypothesis that relatively small changes in oceanic nutrient content can lead to widespread euxinia at the end-Permian. A doubling or tripling of $[PO_4^{3-}]$ can account for Late Permian Panthalassic anoxia, and increases greater than 3× modern values lead to extreme euxinia akin to what has been hypothesized for the extinction interval. The presence of H_2S in surface and deep waters would pose severe environmental stress upon marine eukaryotes. Depending on the concentration and exposure time to H_2S, euxinia would be fatal to most eukaryotes. It is possible, however, for H_2S concentrations to have remained very low for the duration of the extinction. Bambach (2006) pointed out that even very small imbalances in birth and death rate within a species can lead to extinction over a geologically short interval, so periodic killings by H_2S or persistent, sublethal $[H_2S]$ may have exerted enough environmental stress to lead to extinction over ~100 k.y.

Hydrogen sulfide accumulation is biogeochemically inseparable from CO_2 buildup, and both toxins likely worked in concert during the extinction event. Knoll et al. (1996) identified selectivity in the pattern of extinction that could be explained by hypercapnia: sessile, heavily calcifying organisms and organisms unable to actively ventilate the respiratory systems were more susceptible to extinction than other taxa (Bambach, 2006; Knoll et al., 1996). While hypercapnic stress elegantly explains the pattern of end-Permian extinction, anoxia and euxinia likely enhanced the magnitude of extinction (Knoll et al., 2007).

CONCLUSIONS

Earth system modeling supports the hypothesis that extreme euxinia and H_2S eruptions can result from modest changes in the ocean's nutrient content. However, the ocean-atmosphere flux of H_2S predicted here is considerably less than that based on the simple calculations of Kump et al. (2005), further diminishing the catastrophic consequences they predicted for atmospheric chemistry and climate. The spatial distribution of euxinia in surface waters is broadly consistent with end-Permian geochemical

records and provides an improved basis for future model-data comparison. Further work is necessary to constrain the role of the nitrogen cycle in the transition to euxinia, end-Permian paleoproductivity, and the nature of the biological pump during this interval. However, comparisons of these spatially resolved predictions to the rock record will help to constrain the geochemical environment that hosted the end-Permian mass extinction.

ACKNOWLEDGMENTS

Meyer acknowledges support from the Pennsylvania State University–National Science Foundation (NSF) Biogeochemical Research Initiative for Education, Integrative Graduate Education and Research Traineeship (DGE 9972759), and the Pennsylvania State University Krynine Fund. The NSF Geobiology and Environmental Geochemistry program (EAR 0208119) and the National Aeronautics and Space Administration Astrobiology Institute (NNA04CC06A) supported Kump and Meyer. We thank A. Knoll, R. Newton, and J. Kiehl for helpful comments on the manuscript. C. Shields and J. Kiehl (National Center for Atmospheric Research) kindly provided Permian model boundary conditions necessary for GENIE-1.

REFERENCES CITED

Algeo, T.J., Ellwood, B., Nguyen, T.K.T., Rowe, H., and Maynard, J.B., 2007, The Permian-Triassic boundary at Nhi Tao, Vietnam: Evidence for recurrent influx of sulfidic watermasses to a shallow-marine carbonate platform: Palaeogeography, Palaeoclimatology, Palaeoecology, v. 252, p. 304–327, doi: 10.1016/j.palaeo.2006.11.055.

Bambach, R.K., 2006, Phanerozoic biodiversity and mass extinctions: Annual Review of Earth and Planetary Sciences, v. 34, p. 127–155, doi: 10.1146/annurev.earth.33.092203.122654.

Beerling, D.J., Harfoot, M., Lomax, B., and Pyle, J.A., 2007, The stability of the stratospheric ozone layer during the end-Permian eruption of the Siberian Traps: Philosophical Transactions of the Royal Society, Series A–Mathematical Physical and Engineering Sciences, v. 365, p. 1843–1866, doi: 10.1098/rsta.2007.2046.

Berner, R.A., 2005, The carbon and sulfur cycles and atmospheric oxygen from Middle Permian to Middle Triassic: Geochimica et Cosmochimica Acta, v. 69, p. 3211–3217, doi: 10.1016/j.gca.2005.03.021.

Demaison, G.J., and Moore, G.T., 1980, Anoxic Environments and Oil Source Bed Genesis: The American Association of Petroleum Geologists Bulletin, v. 64, p. 1179–1209.

Edwards, N., and Marsh, R., 2005, Uncertainties due to transport-parameter sensitivity in an efficient 3-D ocean-climate model: Climate Dynamics, v. 24, p. 415–433, doi: 10.1007/s00382–004–0508–8.

Erwin, D.H., 2006, Extinction: How Life on Earth Nearly Ended 250 Million Years Ago: Princeton, New Jersey, Princeton University Press, 296 p.

Grice, K., Cao, C.Q., Love, G.D., Bottcher, M.E., Twitchett, R.J., Grosjean, E., Summons, R.E., Turgeon, S.C., Dunning, W., and Jin, Y.G., 2005, Photic zone euxinia during the Permian-Triassic superanoxic event: Science, v. 307, p. 706–709, doi: 10.1126/science.1104323.

Hallam, A., and Wignall, P.B., 1999, Mass extinctions and sea-level changes: Earth-Science Reviews, v. 48, p. 217–250, doi: 10.1016/S0012–8252(99)00055–0.

Hays, L., Love, G.D., Foster, C.B., Grice, K., and Summons, R.E., 2006, Lipid biomarker records across the Permian-Triassic boundary from Kap Stosch, Greenland: Eos (Transactions, American Geophysical Union), v. 87, no. 52, PP41B–1203.

Hays, L.E., Beatty, T., Henderson, C.M., Love, G.D., and Summons, R.E., 2007, Evidence for photic zone euxinia through the end-Permian mass extinction in the Panthalassic Ocean (Peace River Basin, Western Canada): Paleoworld, v. 16, p. 39–50, doi: 10.1016/j.palwor.2007.05.008.

Hotinski, R.M., Bice, K.L., Kump, L.R., Najjar, R.G., and Arthur, M.A., 2001, Ocean stagnation and end-Permian anoxia: Geology, v. 29, p. 7–10, doi: 10.1130/0091–7613(2001)029<0007:OSAEPA>2.0.CO;2.

Huey, R.B., and Ward, P.D., 2005, Hypoxia, global warming, and terrestrial Late Permian extinctions: Science, v. 308, p. 398–401, doi: 10.1126/science.1108019.

Isozaki, Y., 1997, Permo-Triassic boundary superanoxia and stratified superocean: Records from lost deep sea: Science, v. 276, p. 235–238, doi: 10.1126/science.276.5310.235.

Kidder, D.L., and Worsley, T.R., 2004, Causes and consequences of extreme Permo-Triassic warming to globally equable climate and relation to the Permo-Triassic extinction and recovery: Palaeogeography, Palaeoclimatology, Palaeoecology, v. 203, p. 207–237, doi: 10.1016/S0031–0182(03)00667–9.

Kiehl, J.T., and Shields, C.A., 2005, Climate simulation of the latest Permian: Implications for mass extinction: Geology, v. 33, p. 757–760, doi: 10.1130/G21654.1.

Knoll, A.H., Bambach, R.K., Canfield, D.E., and Grotzinger, J.P., 1996, Comparative Earth history and Late Permian mass extinction: Science, v. 273, p. 452–457, doi: 10.1126/science.273.5274.452.

Knoll, A.H., Bambach, R.K., Payne, J.L., Pruss, S., and Fischer, W.W., 2007, Paleophysiology and end-Permian mass extinction: Earth and Planetary Science Letters, v. 256, p. 295–313, doi: 10.1016/j.epsl.2007.02.018.

Krull, E.S., and Retallack, G.J., 2000, $\delta^{13}C$ depth profiles from paleosols across the Permian-Triassic boundary: Evidence for methane release: Geological Society of America Bulletin, v. 112, p. 1459–1472, doi: 10.1130/0016–7606(2000)112<1459:CDPFPA>2.0.CO;2.

Kump, L.R., Pavlov, A., and Arthur, M.A., 2005, Massive release of hydrogen sulfide to the surface ocean and atmosphere during intervals of oceanic anoxia: Geology, v. 33, p. 397–400, doi: 10.1130/G21295.1.

Lamarque, J.F., Kiehl, J.T., and Orlando, J.J., 2007, Role of hydrogen sulfide in a Permian-Triassic boundary ozone collapse: Geophysical Research Letters, v. 34, doi: 10.1029/2006GL028384.

Meyer, K.M., and Kump, L.R., 2008, Oceanic euxinia in Earth history: Causes and consequences: Annual Review of Earth and Planetary Sciences, v. 36, p. 251–288, doi: 10.1146/annurev.earth.36.031207.124256.

Mundil, R., Ludwig, K.R., Metcalfe, I., and Renne, P.R., 2004, Age and timing of the Permian mass extinctions: U/Pb dating of closed-system zircons: Science, v. 305, p. 1760–1763, doi: 10.1126/science.1101012.

Newton, R.J., Pevitt, E.L., Wignall, P.B., and Bottrell, S.H., 2004, Large shifts in the isotopic composition of seawater sulphate across the Permo-Triassic boundary in northern Italy: Earth and Planetary Science Letters, v. 218, p. 331–345, doi: 10.1016/S0012–821X(03)00676–9.

Nielsen, J.K., and Shen, Y., 2004, Evidence for sulfidic deep water during the Late Permian in the East Greenland Basin: Geology, v. 32, p. 1037–1040, doi: 10.1130/G20987.1.

Payne, J.L., Lehrmann, D.J., Wei, J.Y., Orchard, M.J., Schrag, D.P., and Knoll, A.H., 2004, Large perturbations of the carbon cycle during recovery from the end-Permian extinction: Science, v. 305, p. 506–509, doi: 10.1126/science.1097023.

Powers, C.M., and Bottjer, D.G., 2007, Bryozoan paleoecology indicates mid-Phanerozoic extinctions were the product of long-term environmental stress: Geology, v. 35, p. 995–998, doi: 10.1130/G23858A.1.

Pruss, S.B., and Bottjer, D.J., 2004, Late Early Triassic microbial reefs of the western United States: A description and model for their deposition in the aftermath of the end-Permian mass extinction: Palaeogeography, Palaeoclimatology, Palaeoecology, v. 211, p. 127–137, doi: 10.1016/j.palaeo.2004.05.002.

Renne, P.R., and Basu, A.R., 1991, Rapid eruption of the Siberian Traps flood basalts at the Permo-Triassic boundary: Science, v. 253, p. 176–179, doi: 10.1126/science.253.5016.176.

Riccardi, A.L., Arthur, M.A., and Kump, L.R., 2006, Sulfur isotopic evidence for chemocline upward excursions during the end-Permian mass extinction: Geochimica et Cosmochimica Acta, v. 70, p. 5740–5752, doi: 10.1016/j.gca.2006.08.005.

Ridgwell, A., Hargreaves, J.C., Edwards, N.R., Annan, J.D., Lenton, T.M., Marsh, R., Yool, A., and Watson, A., 2007, Marine geochemical data assimilation in an efficient earth system model of global biogeochemical cycling: Biogeosciences, v. 4, p. 87–104.

Van Cappellen, P., and Ingall, E.D., 1994, Benthic phosphorus regeneration, net primary production, and ocean anoxia: A model of the coupled marine biogeochemical cycles of carbon and phosphorus: Paleoceanography, v. 9, p. 677–692, doi: 10.1029/94PA01455.

Wignall, P.B., and Twitchett, R.J., 1996, Oceanic anoxia and the end Permian mass extinction: Science, v. 272, p. 1155–1158, doi: 10.1126/science.272.5265.1155.

Wignall, P.B., and Twitchett, R.J., 2002, Extent, duration, and nature of the Permian-Triassic superanoxic event, *in* Koeberl, C., and MacLeod, K.C., eds., Catastrophic Events and Mass Extinctions: Impacts and Beyond: Geological Society of America Special Paper 356, p. 395–413.

Wignall, P.B., Newton, R., and Brookfield, M.E., 2005, Pyrite framboid evidence for oxygen-poor deposition during the Permian-Triassic crisis in Kashmir: Palaeogeography, Palaeoclimatology, Palaeoecology, v. 216, p. 183–188, doi: 10.1016/j.palaeo.2004.10.009.

Winguth, A.M.E., and Maier-Reimer, E., 2005, Causes of the marine productivity and oxygen changes associated with the Permian-Triassic boundary: A reevaluation with ocean general circulation models: Marine Geology, v. 217, p. 283–304, doi: 10.1016/j.margeo.2005.02.011.

Manuscript received 22 January 2008
Revised manuscript received 15 May 2008
Manuscript accepted 10 June 2008

Printed in USA